

Analysis of angular distributions in $\gamma N \rightarrow \pi^0 \eta N$

A. Fix*, M. Ostrick, and L. Tiator

Institut für Kernphysik, Johannes Gutenberg-Universität Mainz, D-55099 Mainz, Germany

(Dated: December 9, 2018)

Angular distributions in the final state of $\pi^0 \eta$ photoproduction on nucleons are considered. As a formal base the familiar isobar model is used in which the $\pi^0 \eta N$ state is a product of the resonance decay into $\eta \Delta(1232)$ and $\pi S_{11}(1535)$ channels. One of the principal assumptions used is that in the actual energy region the reaction is dominated by a single resonance state. The developed formalism can serve as a tool for testing spin and parity of that resonance.

PACS numbers: 13.40.-f, 13.60.Le, 14.20.Gk

I. INTRODUCTION

Recent measurements [1] of the total cross section for $\pi^0 \eta$ photoproduction off the proton have shown that its value rapidly rises with increasing energy and in the region $E_\gamma > 1.2$ GeV it exceeds the cross section for single η photoproduction. At the same time, already a simple analysis shows that the dynamics of this reaction is by no means trivial. Indeed, calculations made with the Born diagrams, Fig. 1(a-f), give only about 10% of the measured cross section value thus pointing to the crucial role of resonances in this reaction (diagrams (g) and (h) in Fig. 1).

The authors of Ref. [2] have proposed as a dominant mechanism excitation of the resonance $D_{33}(1700)$ with a subsequent decay into the $\eta \Delta(1232)$ channel. It is quite clear that if the role of the Born terms is negligible, then in order to account for the rapid rise of the cross section near threshold, one has no choice but to take a resonance decaying into s -wave $\eta \Delta$ state for which the $D_{33}(1700)$ is a very good candidate.

However, according to the experimental results of Ref. [1], the cross section does not demonstrate a pronounced resonance like energy dependence. It reaches about 4 μb at $E_\gamma = 1.3$ GeV and then does not essentially change at least up to $E_\gamma = 2.2$ GeV. Such a smooth behavior might be due to the fact that the mass of the excited resonance is close or even below the threshold energy, so that the corresponding peak is folded with the increasing reaction phase space. This situation might lead to strong uncertainties in determining the resonance parameters when fitting the cross section. Furthermore we can not exclude the case with two or more strongly overlapping resonance states, having different spin and parity and thus contributing incoherently. To clarify the situation a detailed analysis of partial waves becomes of special importance. Some work in this direction has already been done by the Bonn-Gatchina group [1]. Their method based on the formalism of Ref. [3] has allowed them to analyse the role of different partial waves. According to their results in the region $1.07 \text{ GeV} \leq E_\gamma \leq 1.45 \text{ GeV}$ the dominant contribution comes from the resonances $D_{33}(1700)$ and $D_{33}(1940)$.

The present study deals mainly with the angular dependence of the cross section which is proposed as a sensitive criterion to identify the underlying production mechanism. Obviously, in the event that only one partial wave dominates, the corresponding angular distribution is governed by the lowest powers of sine or cosine of spherical angles, whereas the Born sector, where large amount of partial waves are involved, provide more or less monotonic angular dependence. Therefore, if we are able to separate the shape of the differential cross section associated with pure harmonics we can expect that not only the resonance part of the amplitude can be isolated from the background but that it is also possible to identify the quantum numbers of individual resonance states.

For simplicity as a first step we consider an ideal case when in the actual energy region of energy the amplitude is dominated by only one resonance R and contributions of other waves can be neglected. We put the resonance mass to $M_R = 1.8$ GeV and take the total width $\Gamma_R = 300$ MeV. The quantum numbers, spin and parity J^π , are treated as model parameters. Our aim is to investigate the dependence of the angular distributions on the choice of $R(J^\pi)$ and in this way to study the signature of individual partial waves. Perhaps, the next natural move would be to identify $R(J^\pi)$ with more or less well-established resonance states known, e.g., from the PDG listing [4]. However, within the quite rudimentary state of the database and the theoretical descriptions, such an approach cannot lead to a unique solution.

The paper is organized as follows. First, in Sect. II we briefly describe the formalism of the sequential decay of the resonance R according to the scheme: $R \rightarrow \text{baryon}(\frac{3}{2}^+) + \text{meson}(0^-)$, $\text{baryon}(\frac{3}{2}^+) \rightarrow \text{baryon}(\frac{1}{2}^+) + \text{meson}(0^-)$ and derive expressions for the angular distributions. Then in Sect. III using the assumption of the isobar model

* Permanent address: Laboratory of Mathematical Physics, Tomsk Polytechnic University, 634050 Tomsk, Russia

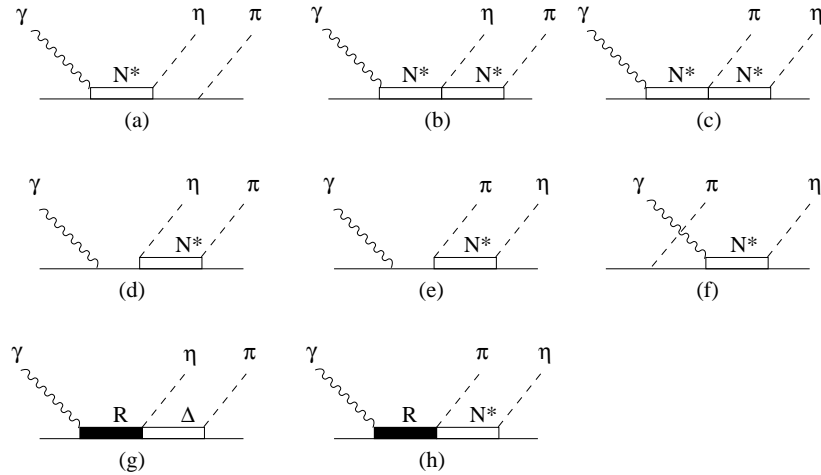


FIG. 1: Diagrams for $\gamma N \rightarrow \pi^0 \eta N$ used in the calculations. The notations Δ and N^* stand for $P_{33}(1232)$ and $S_{11}(1535)$, respectively.

we calculate the angular and energy dependence within different hypotheses about spin-parity of the resonance R . Finally, in Sect. IV we summarize our main qualitative results.

II. ANGULAR DISTRIBUTIONS. FORMALISM.

We consider the process

$$\gamma(\vec{k}) + N_i(-\vec{k}) \rightarrow \pi^0(\vec{q}_\pi) + \eta(\vec{q}_\eta) + N_f(\vec{p}_f), \quad (1)$$

where the 3-momenta of the particles in the overall c.m. frame are given in parenthesis. In general, the resonance mechanism of the reaction (1) can be realized according to the following two schemes (throughout the paper the resonance $S_{11}(1535)$ is denoted by N^*)

$$\begin{aligned} (a) : \gamma N &\rightarrow R(J^\pi) \rightarrow \eta \Delta^+ \rightarrow \pi^0 \eta N, \\ (b) : \gamma N &\rightarrow R(J^\pi) \rightarrow \pi^0 N^* \rightarrow \pi^0 \eta N \end{aligned} \quad (2)$$

(see diagrams (g) and (h) in Fig. 1), the relative amount of which depends on the details of the reaction dynamics. The first scheme with $R = D_{33}(1700)$ was considered in [2] as a main driving mechanism of the reaction (1). The second sequence appears in Ref. [2] due to strong ηN interaction via N^* excitation.

The resonance states R considered in this paper are listed in Table I together with orbital momenta associated with their decay into different channels. Throughout this section we assume that the $\pi^0 \eta$ production always proceeds according to the scheme (a). The scheme (b) will be included in the next section where we present our results obtained within the isobar model.

When writing the resonances in the form L_{2T2J} in Table I we took into account that only the states with isospin $T = 3/2$ decay into the $\eta \Delta$ channel. As already noted, we do not try to identify the states $R(J^\pi)$ with the baryon spectrum known from PDG [4]. But if only the quantum numbers are taken into consideration the states collected in Table I may be identified with, e.g., $S_{31}(1900)$, $P_{31}(1910)$, $D_{33}(1700)$, $P_{33}(1920)$, $D_{35}(1930)$, and $F_{35}(1905)$. These resonances, except for $D_{33}(1700)$, belong to the third group and can influence the low-energy region only through their large widths. It is also worth noting that all the mentioned states are characterized by quite a weak πN mode (generally less than 20 %) and therefore can intensively decay into the two-meson channels.

The kinematics of the reaction (1) is presented in Fig. 2. We select the z -axes along the photon momentum \vec{k} . The production plane is spanned by the momenta \vec{k} and \vec{q}_η , so that $\phi_\eta = 0$. The decay plane of the πN pair is fixed by the momenta \vec{q}_π and \vec{p}_f . We denote by $\Omega = (\theta, \phi)$ the solid pion angle in the πN rest frame. To describe the $\Delta \rightarrow \pi N$ decay, two types of the coordinate systems $Ox'y'z'$ are used. In the first one, the canonical frame (also referred to as Adair frame, Fig. 2(a)), all three axes are codirectional to those of the $OXYZ$ system, so that the system $O'x'y'z'$ is deduced by the Lorentz boost determined by the vector $\vec{q}_\pi + \vec{p}_f$. In the helicity frame (Fig. 2(b)) the z' axis is aligned

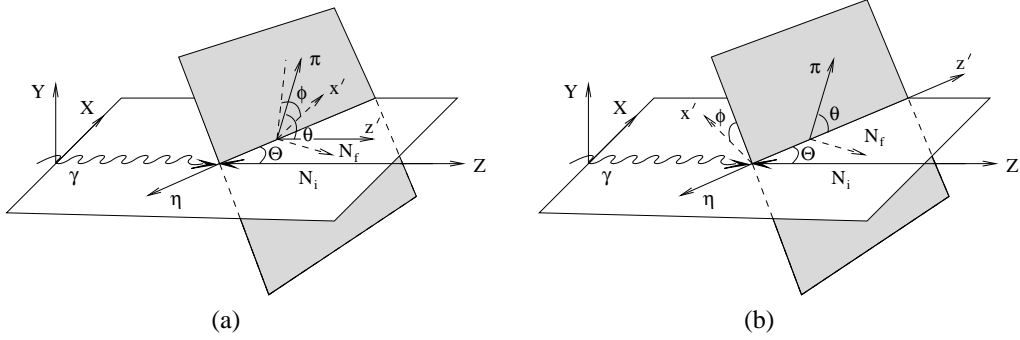


FIG. 2: The angles Θ and $\Omega = (\theta, \phi)$ describing directions of the final particles. The panels (a) and (b) represent configurations of the momenta in the canonical and the helicity systems, referred in the text as K - and H -system, respectively.

TABLE I: Angular momenta associated with a decay of the resonance $R(J^\pi)$ into hadronic channels. In the $\eta\Delta$ states only the lower of two possible values of L is assumed. The resonance $S_{11}(1535)$ is denoted as N^* .

| $J^\pi(L_{2T2J})$ | $L(\pi N)$ | $L(\eta\Delta)$ | $L(\pi N^*)$ |
|-------------------------|------------|-----------------|--------------|
| $\frac{1}{2}^-(S_{31})$ | 0 | 2 | 1 |
| $\frac{1}{2}^+(P_{31})$ | 1 | 1 | 0 |
| $\frac{3}{2}^-(D_{33})$ | 2 | 0 | 1 |
| $\frac{3}{2}^+(P_{33})$ | 1 | 1 | 2 |
| $\frac{5}{2}^-(D_{35})$ | 2 | 2 | 3 |
| $\frac{5}{2}^+(F_{35})$ | 3 | 1 | 2 |

along the vector $\vec{q}_\eta + \vec{p}$ and the x' axis is in the production plane. To shorten the notations we denote by Θ the polar angle of the vector $\vec{p}_\Delta = \vec{q}_\pi + \vec{p} = -\vec{q}_\eta$ in the overall c.m. system, and by $\Omega = (\theta, \phi)$ the pion momentum in the πN rest frame. The coordinate systems above will further be referred as K - and H -system respectively. Clearly, they are connected to each other by a rotation with the angle Θ around the y' axis.

The amplitude associated with the diagram (g) in Fig. 1 has the following form in the canonical and the helicity frame

$$t_{m_f\lambda}^K(\Theta, \Omega) = \frac{1}{\sqrt{4\pi}} \sum_{R(JL)} \alpha^R A_\lambda^R \sum_m \sqrt{2L+1} C_{1m \frac{1}{2}m_f}^{\frac{3}{2}M_\Delta} C_{LM_L \frac{3}{2}M_\Delta}^{J\lambda} Y_{1m}^*(\Omega) d_{M_L 0}^L(\Theta), \quad (3)$$

$$t_{m_f\lambda}^H(\Theta, \Omega) = \frac{1}{\sqrt{4\pi}} \sum_{R(JL)} \alpha^R A_\lambda^R \sum_m \sqrt{2L+1} C_{1m \frac{1}{2}m_f}^{\frac{3}{2}\mu_\Delta} C_{L0 \frac{3}{2}\mu_\Delta}^{J\mu_\Delta} Y_{1m}^*(\Omega) d_{\lambda\mu_\Delta}^J(\Theta). \quad (4)$$

Here, $C_{j_1 m_1 j_2 m_2}^{JM}$ are the usual Clebsch-Gordan coefficients for the coupling $\vec{j}_1 + \vec{j}_2 = \vec{J}$. The index L is the $\eta + \Delta$ orbital momentum and $d_{mm'}^L(d_{\mu\mu'}^J)$ are the rotation matrices. In the second equation μ_Δ stands for the Δ helicity. The spherical function $Y_{1m}(\Omega)$ specifies the angular dependence of the decay $\Delta \rightarrow \pi N$ in the πN rest frame. The index λ is the initial state helicity. Since the momenta of the initial particles are along the Z -axes, the photon helicity is combined with the nucleon helicity to give the z projection of the total angular momentum J equal to $\lambda \in \{\pm 1/2, \pm 3/2\}$. The corresponding amplitude of the transition $\gamma N \rightarrow R(J^\pi)$ is denoted by A_λ^R . Parity conservation requires that

$$A_{-\lambda}^R = (-1)^{\frac{1}{2}+J-l} A_\lambda^R. \quad (5)$$

The parameters α^R characterizing the individual resonances R contain constants and energy dependent functions (resonance propagators, barrier penetration factors, coupling constants, etc.), which detailed structure is irrelevant for further discussions. We note that the nucleon magnetic quantum numbers m_f in (3) and (4) are projections of the final nucleon spin on different z' -axes, according to their definitions in the K - and H -system (see Fig. 2).

Using Eq. (3) or (4) together with (5) it is easy to verify that parity conservation leads to the following symmetry property

$$t_{-m_f-\lambda}^{K/H}(\Theta; \theta, \phi) = (-1)^{m_f-\lambda} t_{m_f\lambda}^{K/H}(\Theta; \theta, -\phi). \quad (6)$$

The square of the matrix element can easily be written down from (3) and (4). Since in this section our main object is the form of angular distributions and not the absolute value of the cross section, it is convenient to introduce the distribution functions, normalized to unity. In the isobar model discussed in the next section we assume that the only nonvanishing contribution to the amplitude comes from the sole state $R(J^\pi)$, whereas other resonances can be neglected. Deriving the formulas below we will always adhere this somewhat oversimplified picture.

First, we consider the distribution over the angle Θ of the πN system in the overall c.m. frame. For this purpose we define the distribution function

$$W(\Theta) = \frac{\pi}{N} \int \sum_{m_f\lambda} |t_{m_f\lambda}(\Theta; \Omega)|^2 d\Omega, \quad (7)$$

$$N = |\alpha^R|^2 \left(|A_{1/2}^R|^2 + |A_{3/2}^R|^2 \right), \quad \int_0^\pi W(\Theta) \sin\Theta d\Theta = 1. \quad (8)$$

Using (3) for a given resonance $R(J^\pi)$ we obtain

$$W(\Theta) = \frac{2L+1}{4(1+a)} \sum_{M_L} |d_{M_L 0}^L(\Theta)|^2 \left(\sum_{\lambda=\pm\frac{1}{2}} (C_{LM_L}^{J\lambda})^2 + a \sum_{\lambda=\pm\frac{3}{2}} (C_{LM_L}^{J\lambda})^2 \right), \quad (9)$$

where the parameter a is defined as

$$a = \left(\frac{A_{3/2}^R}{A_{1/2}^R} \right)^2. \quad (10)$$

As is evident from Eq. (9), the distribution over $\cos\Theta$ is flat for $J^\pi = 1/2^\pm$ since in this case $a = 0$ and $\sum_{\lambda=\pm 1/2} (C_{LM_L}^{J\lambda})^2 = 2/(2L+1)$ does not depend on M_L . The same is true for $L = 0$ which we have in the state with $J^\pi = 3/2^-$ (see Table I). Thus

$$W(\Theta) = \frac{1}{2}, \quad \text{if } J^\pi = \frac{1}{2}^\pm \quad \text{or} \quad J^\pi = \frac{3}{2}^- \quad (L=0). \quad (11)$$

Otherwise the shape of $W(\Theta)$ is described by a polynomial of $\cos\Theta$ of the order $2L$. Table II lists the function $W(\Theta)$ for all six transitions considered here. As is seen from the Eq. (9), the exact form of $W(\Theta)$ depends on the ratio $a = (A_{3/2}^R/A_{1/2}^R)^2$. This fact brings a model dependence into our analysis, especially if the electromagnetic amplitudes A_λ^R are poorly known. On the other hand, for $J^\pi = 5/2^+$ all coefficients in the expansion are positively defined ($a > 0$). As a result, the corresponding distribution will always reach its maximum at $|\cos\Theta| = 1$. For $J^\pi = 3/2^+$ and $J^\pi = 5/2^-$ the shape of the distribution might be quite sensitive to the value of a . In such a situation indirect information about the spin of R can be obtained from the complexity of the angular distribution, which as mentioned before is fixed to $2L$ for $J \geq \frac{3}{2}$.

Now we turn to the Ω dependence at fixed Θ . The corresponding distribution function reads

$$W(\Theta; \Omega) = \frac{1}{N(\Theta)} \sum_{m_f\lambda} |t_{m_f\lambda}(\Theta; \Omega)|^2, \quad (12)$$

where the factor $N(\Theta)$ is determined by the normalization condition

$$\int W(\Theta; \Omega) d\Omega = 1. \quad (13)$$

TABLE II: Distribution $W(\Theta)$ (7) over the angle Θ of the πN system in the overall c.m. frame and the θ distribution $f(\theta) = 2\pi W(\Theta = 0; \theta, \phi)$ (22) of pions produced by the Δ decay in coincidence with η mesons at $\Theta_\eta = \pi$.

| $J^\pi(L_{2T2J})$ | $W(\Theta)$ | $f(\theta)$ |
|-------------------------|--|--|
| $\frac{1}{2}^-(S_{31})$ | $\frac{1}{2}$ | $\frac{1}{4}(1 + 3\cos^2\theta)$ |
| $\frac{1}{2}^+(P_{31})$ | $\frac{1}{2}$ | $\frac{1}{4}(1 + 3\cos^2\theta)$ |
| $\frac{3}{2}^-(D_{33})$ | $\frac{1}{2}$ | $\frac{1}{4(1+a)}(1 + 3a + 3(1-a)\cos^2\theta)$ |
| $\frac{3}{2}^+(P_{33})$ | $\frac{1}{10(1+a)}(7 + 3a - 6(1-a)\cos^2\Theta)$ | $\frac{1}{4(1+9a)}(1 + 27a + 3(1-9a)\cos^2\theta)$ |
| $\frac{5}{2}^-(D_{35})$ | $\frac{3}{28(1+a)}(2 + 7a + 5(4-5a)\cos^2\Theta - 10(2-3a)\cos^4\Theta)$ | $\frac{1}{4(1+6a)}(1 + 18a + 3(1-6a)\cos^2\theta)$ |
| $\frac{5}{2}^+(F_{35})$ | $\frac{3}{20(1+a)}(2 + 3a + (4+a)\cos^2\Theta)$ | $\frac{3}{4(3+2a)}(1 + 2a + (3-2a)\cos^2\theta)$ |

It is convenient to present the function $W(\Theta; \Omega)$ in the form

$$W(\Theta; \Omega) = \sum_{mm'} Y_{1m}^*(\Omega) \rho_{mm'}(\Theta) Y_{1m'}(\Omega), \quad (14)$$

where, e.g., from Eq. (3) the correlation coefficients $\rho_{mm'}(\Theta)$ read

$$\rho_{mm'}(\Theta) = \frac{2L+1}{4\pi N(\Theta)} \sum_{m_f \lambda} \sum_{M_L M'_L} \mathcal{B}_{m_f \lambda, mm'}^{M_L M'_L} d_{M_L 0}^L(\Theta) d_{M'_L 0}^L(\Theta) \quad (15)$$

with

$$\mathcal{B}_{m_f \lambda, mm'}^{M_L M'_L} = \sum_{m_f \lambda} C_{1m \frac{1}{2} m_f}^{\frac{3}{2} M_\Delta} C_{1m' \frac{1}{2} m_f}^{\frac{3}{2} M'_\Delta} C_{LM_L \frac{3}{2} M_\Delta}^{J\lambda} C_{LM'_L \frac{3}{2} M'_\Delta}^{J\lambda} |\alpha^R A_\lambda^R|^2. \quad (16)$$

The unit-trace condition for the matrix $\rho_{mm'}$ immediately follows from the Eqs. (13) and (14)

$$\sum_m \rho_{mm}(\Theta) = 1. \quad (17)$$

It is intuitively clear that the structure of the pion angular distribution will be governed by the Δ spin $J_\Delta = 3/2$ and should contain polynomials of $\cos\theta$ up to the order $2J_\Delta - 1 = 2$. Using Eq. (14) one has

$$\begin{aligned} W(\Theta; \theta, \phi) &= \frac{3}{4\pi} \left(\rho_{00} \cos^2\theta + \frac{1}{2} (\rho_{11} + \rho_{-1-1}) \sin^2\theta - \sin^2\theta (\mathcal{R}e \rho_{1-1} \cos 2\phi - \mathcal{I}m \rho_{1-1} \sin 2\phi) \right. \\ &\quad \left. + \frac{1}{\sqrt{2}} \sin 2\theta \mathcal{R}e (\rho_{-10} - \rho_{10}) \cos\phi - \frac{1}{\sqrt{2}} \sin 2\theta \mathcal{I}m (\rho_{-10} + \rho_{10}) \sin\phi \right), \end{aligned} \quad (18)$$

where we have dropped the argument Θ in $\rho_{mm'}(\Theta)$. In (18) the hermiticity of the matrix $\rho_{mm'}$ was already used. Furthermore from (6) it is evident that all elements $\rho_{mm'}$ are real and $\rho_{-m-m'} = (-1)^{m-m'} \rho_{mm'}$. Taking also into account the normalization condition (17) we arrive at the result that from nine real elements $\rho_{mm'}$ only three, ρ_{00} , ρ_{10} and ρ_{1-1} remain independent so that the distribution function is reduced to

$$W(\Theta; \theta, \phi) = \frac{3}{4\pi} \left(\rho_{00} \cos^2\theta + \frac{1}{2} (1 - \rho_{00}) \sin^2\theta - \sqrt{2} \mathcal{R}e \rho_{10} \sin 2\theta \cos 2\phi - \rho_{1-1} \sin^2\theta \cos 2\phi \right). \quad (19)$$

Projection of (19) on the y' axis gives

$$W(\Theta; \theta = \phi = \frac{\pi}{2}) = \frac{3}{4\pi} \left(\frac{1}{2} (1 - \rho_{00}) + \rho_{1-1} \right). \quad (20)$$

Obviously, this combination is invariant under rotation around the y' axis. In fact, it is proportional to one of three eigenvalues of the matrix ρ (see, e.g., [5]) so that

$$\rho_{00}^H - 2\rho_{1-1}^H = \rho_{00}^K - 2\rho_{1-1}^K, \quad (21)$$

where $\rho_{mm'}^H$ and $\rho_{mm'}^K$ are the correlation coefficients calculated in the H - and K -system.

Equation (19) is the basic equation that will be used in the rest of the paper to evaluate the angular distributions. Its structure is independent of the particular frame chosen for the description of the Δ decay, since it is fixed by the Δ spin and the parity conservation condition (6). The coefficients $\rho_{mm'}(\Theta)$ are determined by the spin-parity of the resonance R . Therefore, analysis of the experimental angular dependence should enable one to get information about the resonance quantum numbers.

A good test of the production mechanisms might be the distribution $W(\Theta; \theta, \phi)$ at $\Theta = 0$, where the Δ decay is observed at forward direction in coincidence with η moving in the opposite direction along the beam axis. Then as follows from Eq. (15) the matrix ρ becomes diagonal and the ϕ dependence in $W(\Theta; \theta, \phi)$ disappears (at $\Theta = 0$ the cross section is obviously invariant under rotation around the Z axis)

$$\begin{aligned} W(\Theta = 0; \theta, \phi) &= \\ &= \frac{3}{4\pi} \left(\rho_{00}(0) \cos^2 \theta + \frac{1}{2} (1 - \rho_{00}(0)) \sin^2 \theta \right) \\ &= \frac{3}{16\pi} \left(\rho_{00}(0) (1 + 3 \cos^2 \theta) + (2 - 3\rho_{00}(0)) \sin^2 \theta \right) \end{aligned} \quad (22)$$

with $\rho_{00}(0) = \rho_{00}(\Theta = 0)$. Using $m = m' = 0$ in (15) we obtain the following formula for $\rho_{00}(0)$

$$\rho_{00}(0) = \frac{2}{3(1+ac)} \quad (23)$$

with

$$c = \left(\frac{C_{L0\frac{3}{2}\frac{3}{2}}^{J\frac{3}{2}}}{C_{L0\frac{3}{2}\frac{1}{2}}^{J\frac{1}{2}}} \right)^2 = 3^{2(1+L-J)} \frac{J + \frac{3}{2}}{J - \frac{1}{2}}, \quad a = \left(\frac{A_{3/2}^R}{A_{1/2}^R} \right)^2. \quad (24)$$

One can readily see from Eqs. (22) to (24) that the first term in Eq. (22), proportional to $1 + 3 \cos^2 \theta$, is provided exclusively by the Δ helicity $\mu_\Delta = 1/2$ whereas the second term with $\sin^2 \theta$ is due to $\mu_\Delta = 3/2$.

The expressions for $f(\theta) = 2\pi W(\Theta = 0; \theta, \phi)$ are summarized in Table II. The situation is particularly simple for $J = 1/2$. In this case $f(\theta)$ does not depend on the electromagnetic part and its form is totally fixed by the Δ spin. It is identical to the angular distribution of pions through the Δ decay in single pion photoproduction. For higher resonances having $J \geq 3/2$, also the substates with the helicity $\mu_\Delta = \pm 3/2$ become populated. As a result, the element ρ_{00} and consequently the shape of $f(\theta)$ depends on the ratio $a = (A_{1/2}^R/A_{3/2}^R)^2$. In particular, it is convex upwards (downwards) in the whole region $-1 \leq \cos \theta \leq 1$ if $ac < 1$ (> 1). According to the formulas in Table II the angular distribution for $J^\pi = 3/2^+$ and $5/2^-$ is convex upwards for not too low values of a . In the other two cases $J^\pi = 3/2^-$ and $5/2^+$ we should observe quite a slight angular dependence with a convex shape downwards for $a < 1$ and $a < 3/2$, respectively. Taking, e.g., $A_{3/2}/A_{1/2} = 0.81$ for $D_{33}(1700)$ from the PDG [4], we obtain $f(\theta) \approx 3 + \cos^2 \theta$.

Besides relatively simple formalism (Eqs. (22) to (24)) the measurement at $\Theta = 0$ has the advantage that at very forward angles Θ the overlap between πN and ηN states becomes minimal. It is especially important at low energies, where the restricted phase space does not allow the particles, e.g., η and Δ to escape the interaction region before the Δ decays. Therefore, this method is a possibility to naturally reduce the corrections appearing when the Δ decay is influenced by the presence of the η meson.

As a next step we consider the distribution over the angles θ and ϕ of the pion momentum in the πN rest frame. First, we introduce a new distribution function defined as

$$\begin{aligned} \widetilde{W}(\Omega) &= \frac{\pi}{N} \int \sum_{m_f \lambda} |t_{m_f \lambda}(\Theta; \Omega)|^2 \sin \Theta d\Theta, \\ &\quad \int \widetilde{W}(\Omega) d\Omega = 1, \end{aligned} \quad (25)$$

with the normalization constant

$$N = |\alpha^R|^2 \left(|A_{1/2}^R|^2 + |A_{3/2}^R|^2 \right). \quad (26)$$

It is clear that the general structure of $W(\Theta; \Omega)$ (19) also holds for $\widetilde{W}(\Omega)$ so that we can immediately write

$$\begin{aligned}\widetilde{W}(\Omega) &= \sum_{mm'} Y_{1m}^*(\Omega) \tilde{\rho}_{mm'} Y_{1m'}(\Omega) \\ &= \frac{3}{4\pi} \left(\tilde{\rho}_{00} \cos^2 \theta + \frac{1}{2} (1 - \tilde{\rho}_{00}) \sin^2 \theta - \sqrt{2} \mathcal{R}e \tilde{\rho}_{10} \sin 2\theta \cos 2\phi - \tilde{\rho}_{1-1} \sin^2 \theta \cos 2\phi \right).\end{aligned}\quad (27)$$

Due to parity conservation the third term in the brackets proportional to $\sin 2\theta$ should vanish, because it changes sign under the transformation $\theta \rightarrow \pi - \theta$, $\phi \rightarrow \phi + \pi$. Therefore $\tilde{\rho}_{10} = 0$ and the matrix $\tilde{\rho}$ has only two independent elements $\rho_0 \equiv \tilde{\rho}_{00}$ and $\rho_1 \equiv \tilde{\rho}_{1-1}$ and is of the form

$$\tilde{\rho} = \begin{pmatrix} \frac{1}{2}(1 - \rho_0) & 0 & \rho_1 \\ 0 & \rho_0 & 0 \\ \rho_1 & 0 & \frac{1}{2}(1 - \rho_0) \end{pmatrix}.\quad (28)$$

It is instructive to consider the eigenvalues α , β , and γ of the matrix $\tilde{\rho}$

$$\begin{aligned}\alpha &= \frac{1}{2}(1 - \rho_0) - \rho_1, \quad \beta = \frac{1}{2}(1 - \rho_0) + \rho_1, \quad \gamma = \rho_0, \\ \alpha + \beta + \gamma &= 1.\end{aligned}\quad (29)$$

The eigenvalue β is proportional to the combination (20) integrated over Θ . From (29) and positive definition of the matrix $\tilde{\rho}$ the following restrictions hold in any reference system

$$0 \leq \rho_0 \leq 1, \quad |\rho_1| \leq \frac{1}{2}(1 - \rho_0).\quad (30)$$

These inequalities can be useful in reconstructing the matrix $\tilde{\rho}$ (28) from the experimental angular distributions on θ and ϕ .

Using Eq. (4) we obtain the following formula for the correlation coefficients in the helicity frame

$$\tilde{\rho}_{mm'}^H = \frac{1}{2N} \sum_{m_f} \sum_{\lambda, \mu, \mu'} \mathcal{A}_{m_f \lambda, mm'}^{\mu \mu'} c_{\lambda, \mu \mu'}^J, \quad \sum_m \tilde{\rho}_{mm}^H = 1,\quad (31)$$

where

$$\mathcal{A}_{m_f \lambda, mm'}^{\mu \mu'} = C_{L0 \frac{3}{2}\mu}^{J\mu} C_{L0 \frac{3}{2}\mu'}^{J\mu'} C_{1m \frac{1}{2}m_f}^{\frac{3}{2}\mu} C_{1m' \frac{1}{2}m_f}^{\frac{3}{2}\mu'} |\alpha^R A_\lambda^R|^2,\quad (32)$$

$$\begin{aligned}c_{\lambda, \mu \mu'}^J &= \frac{2J+1}{2} \int_0^\pi d_{\lambda \mu}^J(\Theta) d_{\lambda \mu'}^J(\Theta) \sin \Theta d\Theta, \\ c_{\lambda, -\mu' - \mu}^J &= c_{\lambda, \mu \mu'}^J.\end{aligned}\quad (33)$$

Substituting $m = m' = 0$ and $m = -m' = 1$ into (31) it is straightforward to obtain the values of ρ_0 and ρ_1 for an individual partial wave $R(J^\pi)$. In particular, the parameter ρ_0 is of very simple form

$$\rho_0^H \equiv \tilde{\rho}_{00}^H = \frac{4}{3} \left(\frac{2L+1}{2J+1} \right) \left(C_{L0 \frac{3}{2}\frac{1}{2}}^{J\frac{1}{2}} \right)^2,\quad (34)$$

so that the diagonal elements of the matrix $\tilde{\rho}$ (28) are totally independent of the electromagnetic part and are fixed only by the spin-parity of the resonance R . For ρ_1^H we have

$$\begin{aligned}\rho_1^H \equiv \tilde{\rho}_{1-1}^H &= \frac{2L+1}{4(1+a)} \sum_{m_f=\pm\frac{1}{2}} \left(\sum_{\lambda=\pm\frac{1}{2}} c_{\lambda, \mu \mu-2}^J + a \sum_{\lambda=\pm\frac{3}{2}} c_{\lambda, \mu \mu-2}^J \right) \\ &\times C_{L0 \frac{3}{2}\mu}^{J\mu} C_{L0 \frac{3}{2}\mu-2}^{J\mu-2} C_{11 \frac{1}{2}m_f}^{\frac{3}{2}\mu} C_{1-1 \frac{1}{2}m_f}^{\frac{3}{2}\mu-2},\end{aligned}\quad (35)$$

or using symmetry properties of the Clebsh-Gordan coefficients and the relation (33) for the coefficients $c_{\lambda, \mu\mu'}^J$,

$$\rho_1^H = \frac{2L+1}{1+a} \frac{1}{\sqrt{3}} \left(c_{\frac{1}{2}, \frac{3}{2} - \frac{1}{2}}^J + a c_{\frac{3}{2}, \frac{3}{2} - \frac{1}{2}}^J \right) C_{L0 \frac{3}{2} \frac{3}{2}}^{J \frac{3}{2}} C_{L0 \frac{3}{2} \frac{3}{2}}^{J - \frac{1}{2}}. \quad (36)$$

Since $c_{\frac{1}{2}, \frac{3}{2} - \frac{1}{2}}^{\frac{1}{2}} = 0$, the resonances with $J^\pi = \frac{1}{2}^\pm$ do not exhibit ϕ dependence. Furthermore, $c_{\frac{3}{2}, \frac{3}{2} - \frac{1}{2}}^{\frac{5}{2}} = 0$, so that for $J = 5/2$ the second term in the brackets, corresponding to the initial helicity state $\lambda = 3/2$, does not contribute. This leads to the fact that the sign of ρ_1 for $J^\pi = 5/2^\pm$ does not depend on the parameter a and therefore the slope of the corresponding ϕ -distribution at $\phi \rightarrow 0$ (or $\phi \rightarrow \pi$) is model independent.

In the canonical system

$$\tilde{\rho}_{mm'}^K = \frac{1}{2N} \sum_{m_f \lambda} \sum_{M_L M'_L} \mathcal{B}_{m_f \lambda, mm'}^{M_L M'_L} c_{M_L M'_L}^L, \quad \sum_m \tilde{\rho}_{mm}^K = 1, \quad (37)$$

where

$$\mathcal{B}_{m_f \lambda, mm'}^{M_L M'_L} = C_{LM_L \frac{3}{2} M_\Delta}^{J\lambda} C_{LM'_L \frac{3}{2} M'_\Delta}^{J\lambda} C_{1m \frac{1}{2} m_f}^{\frac{3}{2} M_\Delta} C_{1m' \frac{1}{2} m_f}^{\frac{3}{2} M'_\Delta} |\alpha^R A_\lambda^R|^2, \quad (38)$$

$$c_{M_L M'_L}^L = \frac{2L+1}{2} \int_0^\pi d_{M_L 0}^L(\Theta) d_{M'_L 0}^L(\Theta) \sin \Theta d\Theta. \quad (39)$$

The elements ρ_0^K and ρ_1^K are then given by

$$\begin{aligned} \rho_0^K &= \frac{1}{2N} \sum_{m_f \lambda M_L} \mathcal{B}_{m_f \lambda, 00}^{M_L M_L}, \\ \rho_1^K &= -\frac{1}{4N} \sum_{m_f \lambda} \left(\mathcal{B}_{m_f \lambda, 1-1}^{-11} + \frac{1}{\sqrt{6}} \sum_{M_L \neq -1} \mathcal{B}_{m_f \lambda, 1-1}^{M_L M_L+2} \right). \end{aligned} \quad (40)$$

Using the last equations one can easily find

$$\rho_0^K = \frac{2}{3(1+a)} \sum_{m_f = \pm \frac{1}{2}} \left(\left(C_{L \frac{1}{2} - m_f \frac{3}{2} m_f}^{J \frac{1}{2}} \right)^2 + a \left(C_{L \frac{3}{2} - m_f \frac{3}{2} m_f}^{J \frac{3}{2}} \right)^2 \right), \quad (41)$$

$$\rho_1^K = -\frac{1}{\sqrt{3}} \left(C_{L-1 \frac{3}{2} \frac{3}{2}}^{J \frac{1}{2}} C_{L1 \frac{3}{2} - \frac{1}{2}}^{J \frac{1}{2}} + \frac{1}{\sqrt{6}} C_{L0 \frac{3}{2} \frac{1}{2}}^{J \frac{1}{2}} C_{L2 \frac{3}{2} - \frac{3}{2}}^{J \frac{1}{2}} + \frac{a}{\sqrt{6}} C_{L0 \frac{3}{2} \frac{3}{2}}^{J \frac{3}{2}} C_{L2 \frac{3}{2} - \frac{1}{2}}^{J \frac{3}{2}} \right). \quad (42)$$

It follows from (42) that the amplitude $A_{3/2}^R$ can contribute to the nondiagonal term ρ_1^K only if $L \geq 2$. In our case this is only $J^\pi = 5/2^-$ (see Table I).

The values $\rho_0^{K/H}$ and $\rho_1^{K/H}$ for all six states are given in Table III. One can see that the combination $\rho_0 - 2\rho_1$ does not change if we turn from the K - to the H -system. This fact becomes trivial if we notice that the equality $\rho_0^H - 2\rho_1^H = \rho_0^K - 2\rho_1^K$ immediately follows from the Eq. (21) after integration over Θ .

Now let us consider the distribution over $\cos \theta$. Its structure is similar to that in the previously discussed case (22)

$$\begin{aligned} \widetilde{W}(\theta) &= \int \widetilde{W}(\theta, \phi) d\phi \\ &= \frac{3}{8} \left(\rho_0 (1 + 3 \cos^2 \theta) + (2 - 3\rho_0) \sin^2 \theta \right). \end{aligned} \quad (43)$$

In analogy to $W(\Theta = 0; \Omega)$ the first and the second terms in Eq. (43), evaluated in the H -system, are related to the Δ helicities $|\mu_\Delta| = 1/2$ and $|\mu_\Delta| = 3/2$, respectively. It is important that in the H -system the element ρ_0^H is independent of a and is totally determined by the quantum numbers of R (see Table III). Furthermore, resonances with different angular momentum and parity contribute incoherently to ρ^H . Therefore, the function $\widetilde{W}(\theta)$ calculated in the helicity frame is especially effective as a tool to identify R .

TABLE III: Coefficients $\rho_0 \equiv \tilde{\rho}_{00}$ and $\rho_1 \equiv \tilde{\rho}_{1-1}$ in Eq.(27) (see also (43) and (44)) calculated in the H - and the K -system.

| $J^\pi(L_{2T2J})$ | $\frac{1}{2}^-(S_{31})$ | $\frac{1}{2}^+(P_{31})$ | $\frac{3}{2}^-(D_{33})$ | $\frac{3}{2}^+(P_{33})$ | $\frac{5}{2}^-(D_{35})$ | $\frac{5}{2}^+(F_{35})$ |
|-------------------|-------------------------|-------------------------|--------------------------------|---------------------------------|------------------------------------|--------------------------------|
| ρ_0^H | $\frac{2}{3}$ | $\frac{2}{3}$ | $\frac{1}{3}$ | $\frac{1}{15}$ | $\frac{2}{21}$ | $\frac{2}{5}$ |
| ρ_1^H | 0 | 0 | $-\frac{1}{6} \frac{1-a}{1+a}$ | $\frac{1}{10} \frac{1-a}{1+a}$ | $\frac{1}{7} \frac{1}{1+a}$ | $-\frac{1}{5} \frac{1}{1+a}$ |
| ρ_0^K | $\frac{1}{3}$ | $\frac{1}{3}$ | $\frac{2}{3} \frac{1}{1+a}$ | $\frac{2}{15} \frac{3+2a}{1+a}$ | $\frac{1}{105} \frac{31+34a}{1+a}$ | $\frac{1}{5} \frac{3+2a}{1+a}$ |
| ρ_1^K | $-\frac{1}{6}$ | $-\frac{1}{6}$ | 0 | $\frac{4}{15} \frac{1}{1+a}$ | $\frac{1}{70} \frac{17+8a}{1+a}$ | $-\frac{1}{10} \frac{1}{1+a}$ |

As for the ϕ dependence of the cross section, its structure follows from the general expression (27)

$$\widetilde{W}(\phi) = \int \widetilde{W}(\theta, \phi) \sin \theta d\theta = \frac{1}{2\pi} (1 - 2\rho_1 \cos 2\phi), \quad (44)$$

where ρ_1 in H - and K -systems are given by the Eqs. (36) and (42). As already pointed out, the ϕ dependence for $\frac{1}{2}^\pm$ is trivial in the helicity system. Furthermore, for the highest resonances with $J^\pi = \frac{5}{2}^\pm$, although the amplitude of the oscillations of \widetilde{W} depends on the parameter a the character of its convexity in the region $0 \leq \phi \leq \pi$ is independent of a . In the K -system, the 3/2-helicity amplitude contributes to ρ_1 only for $J^\pi = 5/2^-$. In the whole, as one can see from Table III, the sign of ρ_1 is fixed only by the spin-parity of the resonance and the character of the ϕ distribution is model independent.

III. ISOBAR MODEL FOR $\gamma N \rightarrow \pi^0 \eta N$. DISCUSSION OF THE RESULTS.

The expressions presented in the previous section relate to the ideal situation where the amplitude for $\gamma N \rightarrow \pi^0 \eta N$ is dominated by the single diagram, Fig. 1(g). The natural question arises: what is the influence of the πN^* channel? Inserting the corresponding diagram, Fig. 1(h), into the formulas above will certainly make them much lengthier and less symmetric. Therefore we consider the problem numerically and discuss in this section the influence of the πN^* production on the results predicted by the formalism of Sect. II. For further study we need a model describing photoexcitation of the state $R(J^\pi)$ and its decay according to the schemes (a) and (b) in Eq.(2). Here we adopt a typical isobar model along the line used for double pion production (see, e.g., [6, 7, 8]).

The amplitude used in the calculation is a sum of the eight terms corresponding to the diagrams in Fig. 1

$$T = T^{(a-f)} + T^{(g)} + T^{(h)}. \quad (45)$$

The first six graphs (a-f) form the background. We neglect the diagrams with ηNN coupling due to its weakness. Therefore, the main model parameters are the partial widths of N^* . We use 45 % for both ηN and πN modes and 10 % for that of $\pi\pi N$. The total width is equal to $\Gamma_{N^*} = 150$ MeV. As already mentioned, the background mechanisms provide only a small fraction of the observed cross section for $\gamma p \rightarrow \eta\pi^0 p$, and this fact is considered as a key indication that the reaction mainly proceeds through resonance excitation. The corresponding amplitudes, depicted in Fig. 1(g-h), read

$$T^{(g)} = T_{\gamma N \rightarrow \eta \Delta} G_\Delta F_{\Delta \rightarrow \pi N}, \quad (46)$$

$$T^{(h)} = T_{\gamma N \rightarrow \pi N^*} G_{N^*} F_{N^* \rightarrow \eta N}, \quad (47)$$

with G_Δ and G_{N^*} standing for the Δ and N^* propagators.

For each resonance $R(J^\pi)$ we used a simple nonrelativistic Breit-Wigner ansatz with an energy-dependent width $\Gamma_R(W)$

$$\begin{aligned} \langle \lambda | T_{\gamma N \rightarrow \eta \Delta} | \vec{q}, M_\Delta \rangle &= A_\lambda^R G_R \langle J\lambda | F_{R \rightarrow \eta \Delta} | \vec{q}, M_\Delta \rangle, \\ \langle \lambda | T_{\gamma N \rightarrow \pi N^*} | \vec{q}, M_{N^*} \rangle &= A_\lambda^R G_R \langle J\lambda | F_{R \rightarrow \pi N^*} | \vec{q}, M_{N^*} \rangle, \\ G_R &= \left(W - M_R + \frac{i}{2} \Gamma_R(W) \right)^{-1}, \quad \lambda = 1/2, 3/2. \end{aligned} \quad (48)$$

The vertices $F_{R \rightarrow x}$ ($x \in \{\eta\Delta, \pi N^*\}$) in Eq. (48) were taken in the phenomenological form

$$\langle JM | F_{R \rightarrow \eta \Delta} | \vec{q}, M_\Delta \rangle = f_{R\eta\Delta} \frac{q^L}{m_\pi^L} C_{LM_L \frac{3}{2}M_\Delta}^{JM} Y_{LM_L}^*(\hat{q}), \quad L = L(\eta\Delta), \quad (49)$$

$$\langle JM | F_{R \rightarrow \pi N^*} | \vec{q}, M_{N^*} \rangle = f_{R\pi N^*} \frac{q^L}{m_\pi^L} C_{LM_L \frac{1}{2}M_{N^*}}^{JM} Y_{LM_L}^*(\hat{q}), \quad L = L(\pi N^*), \quad (50)$$

where $L(\eta\Delta)$ and $L(\pi N^*)$ are given in Table I. As already noted, in (49) we assume only the lower of two possible values of the angular momentum $L(\eta\Delta)$. In both channels (49) and (50) the finite width of the Δ and N^* isobars was taken into account, what is important for the low energies considered here. Significant contribution to the width of each resonance is assumed to come from the $\pi\pi N$ mode (see Eq. (54)). The corresponding energy dependence was taken in a simple form

$$\Gamma_{\pi\pi N}(W) \sim (W - M_N - 2m_\pi) \Theta(W - M_N - 2m_\pi). \quad (51)$$

Since our calculation relates to the region of low kinetic energies we use the nonrelativistic formalism for Δ and N^* states. Therefore, we do not touch upon such a complication as off-shell ambiguity in the $F_{\Delta \rightarrow \pi N}$ vertex in Eq. (46) appearing in the relativistic treatment of the spin 3/2 field (see, e.g., Ref. [9]).

Taking the $R \rightarrow \pi N^*$ transition in the phenomenological form (50) we have essentially simplified the problem in comparison to Ref. [2] where the $D_{33} \rightarrow \pi N^*$ decay is calculated microscopically. Within the approach of Ref. [2] the process $\gamma N \rightarrow D_{33} \rightarrow \eta\Delta$ is treated as a driving mechanism producing the $\pi^0\eta N$ state already at tree level. The coupling constant $f_{R\eta\Delta}$ entering the vertex $R \rightarrow \eta\Delta$ is taken from the analysis of Ref. [10]. Then the production of the πN^* state proceeds as a series of interactions $D_{33} \rightarrow \eta\Delta^+ \rightarrow \pi^0\eta p \rightarrow \pi^0 N^*$, taken up to the first order in the corresponding two-body scattering matrices. In our case, the constant $f_{R\pi N^*}$ in (50) is real and its absolute value is fixed by the unitarity condition which for the Breit-Wigner resonance reads

$$\Gamma_{\pi N^*} = \Gamma_R - \Gamma_{\pi N} - \Gamma_{\pi\pi N} - \Gamma_{\eta\Delta}. \quad (52)$$

The model should be reasonably good at least close to the resonance position $W \approx M_R$. With distance from this point the energy dependence dictated by the Breit-Wigner ansatz (48) could differ from the one obtained within the microscopic approach. Clearly, the most unambiguous treatment would be a three-body calculation including all coupled channels $\pi\pi N$, πN and $\pi\eta N$.

Close to the $\pi\eta$ production threshold, the functions $\Gamma_{\eta\Delta}(W)$ and $\Gamma_{\pi N^*}(W)$ are mainly determined by the centrifugal barrier effect resulting in $\Gamma_x \sim q_x^{2L(x)+1}$, where $x \in \{\eta\Delta, \pi N^*\}$ and the orbital momenta $L(x)$ are collected in Table I. We can expect that in the low energy region the relative fraction of the πN^* channel is important in the $\frac{1}{2}^\pm$ channels since their decaying into $\eta\Delta$ requires higher values of $L(\eta\Delta)$. As already noted, the $\frac{3}{2}^-$ state might be a well candidate to explain the rapid rise of the cross section in the threshold region. Another state producing s -waves in the $\pi\eta N$ system is $\frac{1}{2}^+$. Any appreciable amount of other states is less likely since their decay into $\pi\eta N$ at low energies is suppressed by the centrifugal barrier.

In Fig. 3 we show an example of the total cross section calculated with $J^\pi = \frac{3}{2}^-$. The calculation demonstrates a strong dominance of the resonance mechanism over the background terms (dashed curve). This result agrees with that of Ref. [2].

For the helicity amplitudes of $D_{33}(1700)$ we used average values [4]

$$A_{1/2} = 0.104 \text{ GeV}^{-1/2}, \quad A_{3/2} = 0.085 \text{ GeV}^{-1/2}, \quad (53)$$

and for the mass and widths

$$\begin{aligned} M_R &= 1.72 \text{ GeV}, \quad \Gamma_R = 300 \text{ MeV}, \quad \frac{\Gamma_{\pi N}}{\Gamma_R} = 20\%, \\ \frac{\Gamma_{\pi\pi N}}{\Gamma_R} &= 73\%, \quad \frac{\Gamma_{\eta\Delta}}{\Gamma_R} = 5\%, \quad \frac{\Gamma_{\pi N^*}}{\Gamma_R} = 2\%, \end{aligned} \quad (54)$$

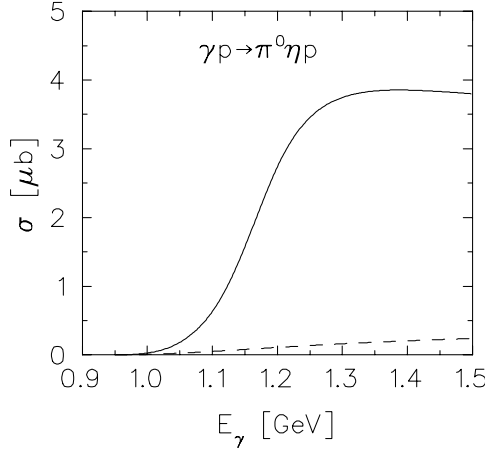


FIG. 3: Total cross section for $\gamma p \rightarrow \pi^0 \eta p$. The dashed curve is the background contribution (diagrams (a) to (f) in Fig. 1).

where all Γ 's are taken at $W = M_R$. The last three values were chosen simply by adjusting the resulting total cross section for $\gamma p \rightarrow \pi^0 \eta p$ to the data of Ref. [1]. It is remarkable that fitting the cross section may require quite a small strength of $D_{33}(1700)$ decay into the $\eta\Delta$ and πN^* channels. In order to get a feeling of possible variation of $\Gamma_{\eta\Delta}$ and $\Gamma_{\pi N^*}$ one can use the formula for the total cross section at the resonance position

$$\sigma(M_R) = C_T(2J+1) \frac{\pi}{k^2} \frac{\Gamma_{\gamma N} \Gamma_{\pi \eta N}}{\Gamma_R^2}, \quad (55)$$

where all energy dependent quantities are calculated at $W = M_R$. The coefficient C_T takes into account the isospin structure and $\Gamma_{\gamma N}$ is the radiation decay width. Taking for $D_{33}(1700)$: $C_T=4/9$, $M_R = 1.7$ GeV, $\Gamma_R = 300$ MeV, and $\Gamma_{\gamma N}/\Gamma_R = 0.19\%$ from [4] we obtain

$$\frac{\Gamma_{\pi \eta N}}{\Gamma_R} \approx 8.5 \cdot 10^{-2} \sigma(M_R). \quad (56)$$

Since around the total energy $W = 1.7$ GeV the cross section has a strong rise the ratio (56) is very sensitive to M_R . For instance, for $M_R = 1.72$ GeV we will have $\sigma(M_R) \approx 0.8 \mu\text{b}$ and $\Gamma_{\pi \eta N} = 7\% \Gamma_R$. The maximum value $\sigma \approx 4 \mu\text{b}$ [1] gives about 34% for the total $\pi\eta N$ width. Then the inequality

$$\Gamma_{\eta\Delta} + \Gamma_{\pi N^*} \leq \Gamma_{\pi \eta N} = 0.34 \Gamma_R \quad (57)$$

holding for the constructive interference between $\eta\Delta$ and πN^* configurations gives an upper limit for the sum of the partial decay widths in $\eta\Delta$ and πN^* .

In the following we discuss a general case in which a resonance $R(J^\pi)$ produces $\pi\eta N$ according to the two schemes in Eq. (2) and the background is totally neglected. For each resonance $R(J^\pi)$ we use the same parameters

$$\begin{aligned} M_R &= 1.8 \text{ GeV}, & \Gamma_R &= 300 \text{ MeV}, & \frac{\Gamma_{\pi N}}{\Gamma_R} &= 20\%, \\ \frac{\Gamma_{\pi\pi N}}{\Gamma_R} &= 60\%, & \frac{\Gamma_{\eta\Delta}}{\Gamma_R} &= 20\%, & \frac{\Gamma_{\pi N^*}}{\Gamma_R} &= 10\%. \end{aligned} \quad (58)$$

For the ratio a (10) we take

$$a \equiv \left(\frac{A_{3/2}}{A_{1/2}} \right)^2 = 0.67. \quad (59)$$

Firstly, we show in Fig. 4 the πN invariant mass spectrum where the contributions of the final state configurations $\eta\Delta$ and πN^* (schemes (a) and (b) in Eq. (2)) are separately presented. It is interesting that the overlap of these states essentially differs in different partial waves. It is quite large in $J^\pi = \frac{3}{2}^-$ and $\frac{5}{2}^+$ and less essential in other waves. Clearly, the character of the interference depends on the particular values of the orbital momenta $L(\eta\Delta)$ and $L(\pi N^*)$ as well as on the relative sign of the $R\eta\Delta$ and $R\pi N^*$ coupling constants.

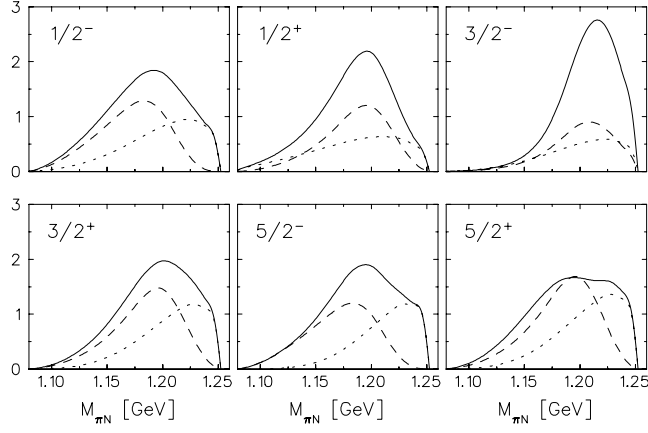


FIG. 4: Distribution of the πN invariant mass calculated at the total γN c.m. energy $W = 1.8$ GeV (corresponds to the photon lab energy about 1.255 GeV). The dashed and the dotted lines show the contribution from the $\eta\Delta$ and πN^* production. The solid line is the coherent sum of both channels. The results are presented in arbitrary units.

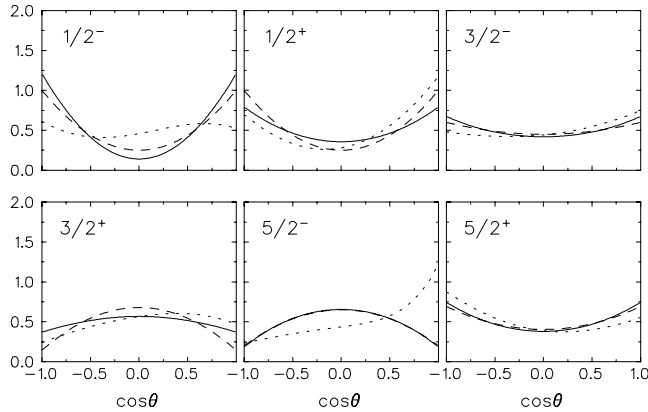


FIG. 5: Angular distributions $f(\theta) = W(\Theta = 0; \theta, \phi)$ of π mesons in the πN c.m. system when the angle Θ is fixed to $\Theta = 0$. The dashed curve contains only the contribution of the driving $\eta\Delta$ term in $R \rightarrow \pi\eta N$ decay (the channel (a) in Eq. (2)). In the dotted curve also the πN^* channel ((b) in Eq. (2)) is taken into account. The solid curve represents the symmetrized function $f_S(\theta)$ (see Eq. (60)) where in addition the invariant πN energy is restricted to the region $M_{\pi N} < 1.13$ GeV. The total γN c.m. energy is $W = 1.8$ GeV.

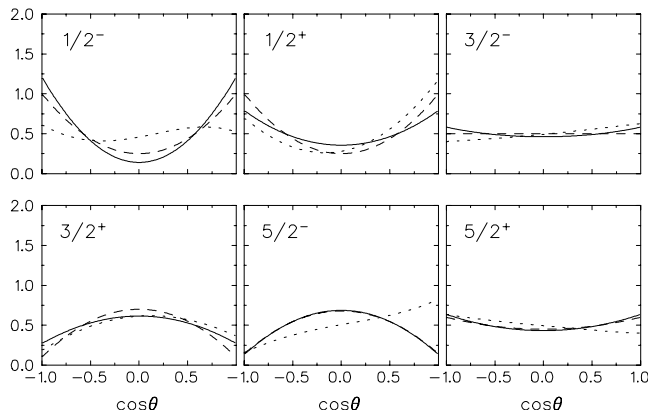


FIG. 6: Distribution $\widetilde{W}(\theta)$ (Eq. (43)) over the polar pion angle in the πN rest frame calculated in the helicity system at $W = 1.8$ GeV. Notation of the curves as in Fig. 5.

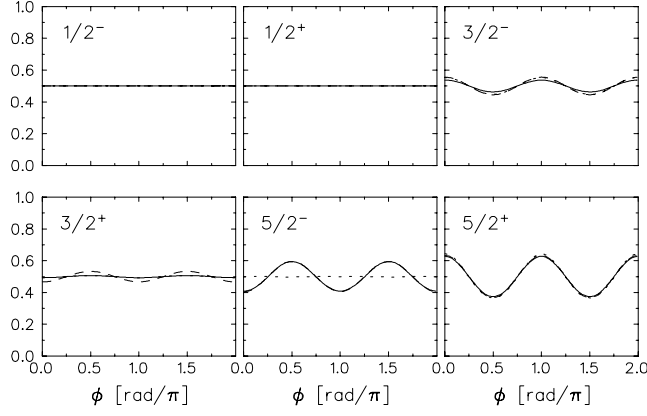


FIG. 7: Distribution $\pi\widetilde{W}(\phi)$ (Eq. (44)) over the azimuthal pion angle in the πN rest frame calculated in the helicity system at $W = 1.8$ GeV. Notation of the curves as in Fig. 5.

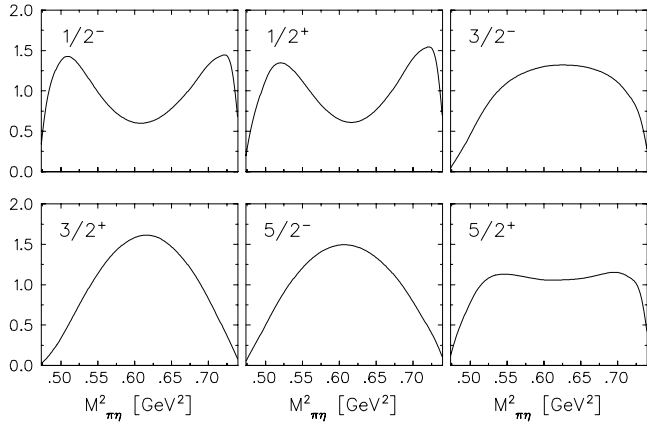


FIG. 8: $\pi^0\eta$ invariant mass spectrum at $W = 1.8$ GeV for different transitions listed in Table I in arbitrary units. The results are obtained without taking the πN^* channel into account.

Of special importance for us is the contribution of the πN^* state in the region of the low invariant masses $M_{\pi N}$. As we can see in Fig. 4 it is important in $\frac{1}{2}^+$ and $\frac{3}{2}^-$ states and can be neglected in other waves if sufficiently low values of $M_{\pi N}$ are considered. Therefore, to isolate the dynamics related to the scheme (a) in Eq. (2) we only need to exclude the region with $M_{\pi N}$ larger than a certain value $M_{\pi N}^0$ depending on the overall reaction energy W . Then it is reasonable to assume that the Δ life time is sufficient to escape interaction with the η meson. In the waves with $J^\pi = \frac{1}{2}^+$ and $\frac{3}{2}^-$ the situation is more complicated at least at the energy $W = 1.8$ GeV considered here. Clearly the overlap between $\eta\Delta$ and πN^* should decrease with increasing W .

In the series of figures 5 to 7 we present examples of angular distributions for $\pi^0\eta$ photoproduction by unpolarized photons on an unpolarized nucleon. The calculation is performed at $W = 1.8$ GeV. In all figures the dashed curve represent the distribution, in which only the channel (a) in Eq. (2) is taken into account. Their form is described by the analytic expressions obtained in Sect. II. Addition of the scheme (b) gives the dotted curve and the solid curve is obtained after cutting off the kinematical region with $M_{\pi N} \geq M_{\pi N}^0 = 1.13$ GeV. As expected, the interference between the channels (a) and (b) tends to distort simple angular dependence, obtained if only the scheme (a) is used. After eliminating the energy region in which both mechanisms strongly overlap, we bring the calculation back to qualitative agreement with the results shown by the dashed curves. This effect is observed in all waves except for $J^\pi = \frac{1}{2}^+$ and $\frac{3}{2}^-$ in accord with our notion about strong overlap of the $\eta\Delta$ and πN^* configurations in these states. In the whole, using the above procedure the qualitative features of the resulting angular distributions are in agreement with the simplified calculations, in which the πN^* channel is neglected.

The solid curve in Fig. 5 contains symmetrization with respect to $\cos \theta = 0$, i.e.

$$f(\theta) \rightarrow f_S(\theta) = \frac{1}{2} (f(\theta) + f(\pi - \theta)). \quad (60)$$

In general, after addition of the channel πN^* the resulting angular dependence yields certain forward-backward asymmetry, which can make the analysis more complicated. This effect is removed after the artificial symmetrization (60).

The θ -distribution in Fig. 6 is quite similar to the one in Fig. 5. As already noted the convex up and down form of $\widetilde{W}(\theta)$ related to $\sin^2 \theta$ and $(1 + 3 \cos^2 \theta)$ terms in Eq. (22) is provided by the Δ helicities $|\mu_\Delta| = 3/2$ and $|\mu_\Delta| = 1/2$. Flat distribution for $J^\pi = \frac{3}{2}^-$ is due to the fact that in this instance (after integration over $\cos \Theta$) we have an even mixture of both helicity states so that the sum of $\frac{1}{3}(1 + 3 \cos^2 \theta)$ and $\sin^2 \theta$ gives a constant value. In other words, in the H -system the longitudinal Δ polarization (averaged over the region $-1 \leq \cos \Theta \leq 1$) is zero if $J^\pi = 3/2^-$. In the case of a small admixture of the πN^* background under the Δ peak we will have an interference term proportional to $\cos \theta$ caused by different parities of N^* and Δ . This effect is clearly seen in Fig. 6 (dotted line in the panel for $J^\pi = \frac{3}{2}^-$). In other cases addition of the πN^* channel leads to more complicated form of the function $\widetilde{W}(\theta)$.

Knowledge of the angular distribution $\widetilde{W}(\theta)$ in the helicity system is of key importance for understanding the spectrum of the $\pi\eta$ pairs. Indeed, for each mass $M_{\pi N}$ the value of $\cos \theta$ ($\theta \equiv \theta_\pi^*$) is determined by $M_{\pi\eta}$ [11] according to

$$\cos \theta = \frac{1}{4WM_{\pi N}q_\pi^*q_\eta} \left[(M_{\pi N}^2 - M_N^2 + m_\pi^2)(W^2 - M_{\pi N}^2 - m_\eta^2) - 2M_{\pi N}^2(M_{\pi\eta}^2 - m_\pi^2 - m_\eta^2) \right], \quad (61)$$

Therefore, the knowledge of $\widetilde{W}(\cos \theta)$ at fixed $M_{\pi N}$ immediately provides the Dalitz plot distribution $d^2\sigma/dM_{\pi N}dM_{\pi\eta}$, and for the $\pi\eta$ spectrum we have

$$\frac{d\sigma}{dM_{\pi\eta}^2} = \int \frac{d^2\sigma}{dM_{\pi N}d\cos \theta} \frac{M_{\pi N}}{2Wq_\pi^*q_\eta} dM_{\pi N}. \quad (62)$$

In other words, if there are no nearby resonances in the $\pi\eta$ system (as in our case), the structure of the Dalitz plot $(M_{\pi N}, M_{\pi\eta})$ is totally determined by the quantum numbers of the resonance R related to its decay into the $\eta\Delta$ and the πN^* channels. In Fig. 8 we present the spectrum $d\sigma/dM_{\pi N}^2$ given by different states $R(J^\pi)$. As we can see, apart from the boundary of the allowed kinematical region where $d\sigma/dM_{\pi\eta}^2 \rightarrow 0$ the spectrum qualitatively reproduces the shape of the angular distribution in the helicity system (dashed curve in Fig. 6). Thus the $\pi\eta$ mass distribution should be sensitive to the quantum numbers of the resonance R . Again for $J^\pi = 1/2^\pm$ the spectrum, having a visible minimum in the middle part is independent of the electromagnetic properties of the resonance. For other resonances it depends on the parameter $a = (A_{1/2}^R/A_{3/2}^R)^2$.

As for the invariant mass distribution in other two-body subsystems, the corresponding measurements can hardly give useful information. As an example, we can take $d\sigma/dM_{\pi N}$ shown in Fig. 4. First of all, the general structure is quite insensitive to the choice of $R(J^\pi)$. If we change from one resonance to another, in the main only the position of the maximum is shifted. Obviously, this shift is explained by the barrier effects. Namely, since $d\sigma/dM_{\pi N} \sim d\sigma/dq_\eta$, for low values of q_η the spectrum is proportional to $q_\eta^{2L(\eta\Delta)+1}$, where $L(\eta\Delta)$ is the angular momentum of the decay $R \rightarrow \eta\Delta$ (see Table I). With increasing $L(\eta\Delta)$ the centrifugal barrier factor tends to suppress the cross section at low q_η (large $M_{\pi N}$), resulting in shifting the maximum to higher values of q_η (lower $M_{\pi N}$). This trivial effect is what we mainly observe in Fig. 4. Furthermore, at higher energies the shape of the spectrum around $M_{\pi N} = M_\Delta$ will be governed by the πN energy distribution in the Δ region, so that the values of $d\sigma/dM_{\pi N}$ is mainly determined by the form of the Δ peak. In this connection, investigation of $d\sigma/dM_{\pi N}$ is not of any use to get additional information on the reaction mechanism.

IV. CONCLUSION

We have discussed some details of a phenomenological analysis of $\gamma N \rightarrow \pi^0 \eta N$ aimed at identifying the dominant mechanisms of this reaction. This analysis assumes that the part of the amplitude corresponding to a given resonance R is sufficiently large, so that other partial waves and the background can be neglected. This assumption seems to be justified by direct calculation of the most important Born diagrams (see Fig. 1). Our results show that even in the absence of the polarization data some interesting properties of the reaction can be found. Our main focus is on the angular dependence as a test of the mechanism responsible for $\pi^0 \eta$ photoproduction. Here we summarize the most important qualitative features of different types of the angular distributions considered in the main part of the paper.

1) The distribution $W(\Theta)$ over the polar angle of the πN system in the γN c.m. frame (Table II). In the simplest case of $J^\pi = \frac{1}{2}^\pm$ we have $W(\Theta) = \text{const}$. Generally, the distribution on Θ depends on the parameter $a = (A_{3/2}/A_{1/2})^2$, which hampers the analysis if the electromagnetic properties of the resonance are poorly known. Indirect clues to the spin-parity of the resonance can be gained from the complexity of $W(\Theta)$. For a state with $\eta\Delta$ angular momentum L the complexity of the $W(\Theta)$ is fixed to $2L$ for $J \geq \frac{3}{2}$.

2) The distribution over $\cos\theta$ at fixed $\Theta = 0$ (Fig. 5). If we select η mesons produced opposite in the direction to the photon beam, a simple formula (23) can be obtained. In the general case the reaction mechanism is such that the intermediate Δ states with both helicities $|\mu_\Delta| = 1/2$ and $3/2$ are populated. As a result, the decay angular distribution of Δ differs from the simple form $1 + 3\cos^2\theta$, peculiar for single pion photoproduction. The weight of each μ_Δ configuration depends on $R(J^\pi)$ so that the method should allow the quantum numbers of R to be extracted from the measurements. As in the $W(\Theta)$ case, the particular form of the distribution in the states with $J^\pi = \frac{3}{2}^+$ and $\frac{5}{2}^\pm$ depends on the value of the parameter a , Eq. (10). However, in a wide range of a , $a > \frac{1}{9}$ for $J^\pi = \frac{3}{2}^+$ and $a > \frac{1}{6}$ for $J^\pi = \frac{5}{2}^-$, the corresponding distributions are not very sensitive to a .

3) The distributions $\widetilde{W}(\theta)$ and $\widetilde{W}(\phi)$ over the polar and azimuthal pion angles in the πN rest frame. For convenience, we express the functions $\widetilde{W}(\theta)$ and $\widetilde{W}(\phi)$ in terms of the Δ decay correlation coefficients $\rho_{mm'}$. Their values can be determined by fitting the analytic expressions for \widetilde{W} to the experimental data.

For $\widetilde{W}(\theta)$ the helicity system (Fig. 6) seems to be more useful for the partial wave analysis since the decay correlation coefficients $\rho_{mm'}^H$ and the corresponding angular distributions are independent of a . Furthermore, there is no interference between partial waves with different spin-parity J^π , so that resonances contribute incoherently. This is especially important in the situation of strongly overlapping states, which is quite typical in the second and the third resonance region. However, there is a sensitivity of the angular distributions to even small admixtures of the πN^* channel. Furthermore, in this case there are qualitative difficulties in distinguishing between the states belonging to the two groups $J^\pi = 1/2^\pm, 5/2^+$ and $J^\pi = 3/2^\pm, 5/2^-$.

The distribution $\widetilde{W}(\phi)$ in the H -system for $J^\pi = \frac{3}{2}^\pm$ seems to be sensitive to the parameter a , Eq. (10). This shortcoming is however partially avoided in the canonical frame where the sign of the ϕ -dependent term does not depend on a .

It has also been shown that if the correlation coefficients ρ_{00}^H (34) are fitted to the data, the spectrum $d\sigma/dM_{\pi N}$ does not provide additional information, since the Dalitz plot is immediately obtained if the distribution over $\cos\theta$ in the H -system is known. This result is a trivial consequence of a linear relation between the cosine of the pion decay angle and $M_{\pi\eta}^2$ (see Eq. (61)).

In general, our results demonstrate that different assumptions about the spin-parity of the dominating partial wave lead to different predictions regarding angular distributions, so that each state R shows its own signature. Model independence of some of these signals as predicted by the present analysis is the major motivation for proposing our method. Additional important information can be obtained from the polarization experiments.

Finally, we would like to note, that the presented calculations are related to the case when most of the $\pi^0\eta N$ configurations are produced through the $R \rightarrow \eta\Delta$ decay. On the other hand, rather low percentage of $\eta\Delta$ and πN^* channels in Eq. (54) indicates that the the measured cross section [1] may be accounted for with quite a small fraction of $\eta\Delta$ and πN^* channels in the total resonance width. This observation might be a reason to doubt the necessity of introducing direct $R\eta\Delta$ coupling to explain $\pi^0\eta$ production rate. The needed strength can be provided by the $R \rightarrow \pi\Delta$ and $R \rightarrow \rho N$ decays followed by $\pi N \rightarrow \eta N$ rescattering. In this case we do not need to restrict ourself to the resonance states with the isospin $T = 3/2$. Clearly, another assumption about the reaction mechanism, as to the one in which the πN^* dominates, will lead to angular distributions different from those presented here.

Acknowledgment

The work was supported by the Deutsche Forschungsgemeinschaft (SFB 443) and by the RF Presidential Grant (No MD-2772.2007.2).

[1] I. Horn, PhD thesis, Universität Bonn, Bonn (2004).
[2] M. Doring, E. Oset, and D Strottman, Phys. Rev. C **73**, 045209 (2006).
[3] A. V. Anisovich, *et al.*, J. Phys. G **28**, 15 (2002).
[4] W. M. Yao *et al.* [Particle Data Group], J. Phys. G **33**, 1 (2006).
[5] J. T. Donohue and H. Högaasen, Phys. Lett. B **25**, 554 (1967).

- [6] J. A. Gomez Tejedor and E. Oset, Nucl. Phys. A **600**, 413 (1996).
- [7] K. Ochi, M. Hirata and T. Takaki, Phys. Rev. C **56**, 1472 (1997).
- [8] A. Fix and H. Arenhövel, Eur. Phys. J. A **25**, 115 (2005).
- [9] R. M. Davidson, N. C. Mukhopadhyay, and R. S. Wittman, Phys. Rev. D **43**, 71 (1991).
- [10] S. Sarkar, E. Oset, and M. J. Vicente Vacas, Nucl. Phys. A **750**, 294 (2005).
- [11] E. Byckling and K. Kajantie, *Particle Kinematics*, Wiley, N.Y. (1973).